Available online at website: https://journal.bcrec.id/index.php/bcrec

Bulletin of Chemical Reaction Engineering & Catalysis, 21 (2) 2026, 274-286

Original Research Article

Hybrid TiO_2@SiO_2 Green Hydrogel Nanocatalyst for High-efficiency Photocatalytic Oxidation of Ciprofloxacin under UV Irradiation: Experimentation and RSM Optimization

Riad Mansour[1,2], Nacer Ferrah[1,3], Nurul Hidayati Fithriyah[4,*], Irfan Purnawan[4], Mustapha Chabane[1], Fadila Zahouane[3], Chikh Melkaoui[5]

[1]University of Naama, BP 66, Naama, Algeria.
[2]Laboratory of Materials Chemistry, University of Oran, BP 1524 El-Menouer, Oran, Algeria.
[3]Laboratory of Inorganic Chemistry and Environment, University of Tlemcen, BP 119,13000-Tlemcen, Algeria.
[4]Chemical Engineering Department, Universitas Muhammadiyah Jakarta, Jakarta Pusat 10510, Indonesia.
[5]Scientific and Technical Research Center on Arid Regions (CRSTRA), Biskra, Algeria.

Received: 1st January 2026; Revised: 25th January 2026; Accepted: 27th January 2026
Available online: 13th February 2026; Published regularly: August 2026

Abstract

A TiO_2@SiO_2 hydrogel nanocomposite was synthesized via a green sol-gel route for the photocatalytic degradation of ciprofloxacin using a UVA/H_2O_2 system. The catalyst was optimized via RSM (response surface methodology), identifying UVA irradiation (365 nm) and pH of 5.6 as key parameters, achieving >89% degradation within 180. Characterisation confirmed homogeneous TiO_2 dispersion within a porous SiO_2 matrix. Kinetics followed a pseudo-first-order Langmuir–Hinshelwood model, and the catalyst retained high activity over five reuse cycles. This study introduces a UVA-optimized, RSM-guided photocatalytic system using a green-synthesized TiO_2@SiO_2 hydrogel – distinguished by its integrated process design, operational simplicity, and focus on solar-compatible UVA rather than conventional UVC-driven TiO_2@SiO_2 systems.

Keywords: Advanced Oxidation Process (AOP); Ciprofloxacin Degradation; Photocatalysis; Response Surface Methodology (RSM); TiO2@SiO2 Nanocomposite

How to Cite: Mansour, R., Ferrah, N., Fithriyah, N. H., Purnawan, I., Chabane, M., Zahouane, F., Melkaoui, C. (2026). Hybrid TiO_2@SiO_2 Green Hydrogel Nanocatalyst for High-efficiency Photocatalytic Oxidation of Ciprofloxacin under UV Irradiation: Experimentation and RSM Optimization. *Bulletin of Chemical Reaction Engineering & Catalysis*, 21 (2), 274-286. (DOI: 10.9767/bcrec.20615)

Permalink/DOI: https://doi.org/10.9767/bcrec.20615

1. Introduction

It is estimated that over 75% of pharmaceutical compounds administered are ultimately released into the environment, primarily via effluents from wastewater treatment plants (WWTPs) [1,2]. Pharmaceutical residues, particularly antibiotics such as ciprofloxacin, persist in aquatic environments due to the limited removal efficiency of conventional wastewater treatment methods [3-5]. Their persistence presence even as low as nanograms per liter [6-11] poses significant ecological and public health risks [12-14], including the promotion of antibiotic resistance genes (ARGs) [15-20]. The inefficiency of antibiotic removal stems from the recalcitrant nature and complex chemical structures of these compounds, which resist conventional biodegradation and physical removal processes [21].

Advanced oxidation processes (AOPs), especially photocatalysis through the generation of reactive oxygen species (ROS), offer a promising alternative by enabling the complete degradation of organic pollutants without secondary contamination [22-24]. TiO_2-based photocatalysts are widely studied for this purpose, yet they often suffer from rapid charge recombination and poor stability [25]. Incorporation of SiO_2 as a support can enhance surface area and stability, though many reported TiO_2/SiO_2 systems still rely on

* Corresponding Author.
Email: nurul.fithriyah@umj.ac.id (N.H. Fithriyah)

high-energy UVC irradiation (254 nm) and lack systematic process optimization [26]. Furthermore, few studies integrate green synthesis, multi-parameter optimization, and catalyst reusability into a single, sustainable treatment framework.

Sol-gel synthesis route is commonly selected in the photocatalyst synthesis for its potential sustainability advantages over conventional high-temperature solid-state methods [27]. Specifically, a green sol-gel protocol is characterized by its low thermal budget (gelation and crystallization at temperatures ≤ 400 °C significantly reduce energy input), benign solvent system (utilization of ethanol and water as primary solvents avoids toxic organic media), and minimized waste (the molecular-level mixing of precursors ensures high product yield and stoichiometric accuracy, reducing material waste) [28]. While traditional sol-gel can involve hazardous alkoxides, this synthesis prioritizes safer handling and aims to minimize the overall environmental footprint of the catalyst fabrication process.

Under UV irradiation, a TiO_2@SiO_2 catalyst generates electron-hole pairs, which react with H_2O/O_2 to produce hydroxyl radicals (•OH). These radicals non-selectively oxidize ciprofloxacin via ring cleavage, defluorination, and decarboxylation, ultimately leading to mineralization into CO_2, H_2O, and inorganic ions (F^-, NO_3^-, NH_4^+) [29]. Despite the importance of UV lights utilization for photocatalytic antibiotic degradation, there have been limited studies in this subject [30] and there are more studies utilizing visible lights irradiation [6,7,22,31-33].

Herein, we report a green-synthesized TiO_2@SiO_2 hydrogel nanocomposite for the photocatalytic degradation of ciprofloxacin using a UVA/H_2O_2 system (Figure 1). Unlike previous TiO_2@SiO_2 studies, this work employs response surface methodology (RSM) to systematically optimize key operational parameters, including UV wavelength (365 nm vs. 254 nm), pH, time, and temperature, while emphasizing solar-compatible UVA-driven performance. The catalyst demonstrates enhanced stability and reusability, and degradation kinetics are modeled using a pseudo-first-order Langmuir–Hinshelwood approach. This study thus presents an integrated, optimized, and sustainable photocatalytic system that advances the design of practical, energy-efficient water treatment technologies.

2. Materials and Methods

2.1 Chemicals

Titanium(IV) isopropoxide (TTIP, 99%), ethanol (99%), 2-propanol (99%), and tetraethoxysilane (TEOS, 98%) were procured from Sigma-Aldrich. Polyethylene glycol (PEG, 99.5%) and ciprofloxacin (98%) were obtained from Merck. Hydrochloric acid (HCl) and sodium hydroxide (NaOH), used for pH adjustments, were supplied by Fluka. Ultrapure water (resistivity 18.2 MΩ·cm) was used exclusively as the solvent throughout all experiments. The ultrapure water is considered a green solvent due to its safety and abundance, while ethanol is a relatively green solvent owing to its low toxicity and potential renewable origin. Ciprofloxacin stock and working

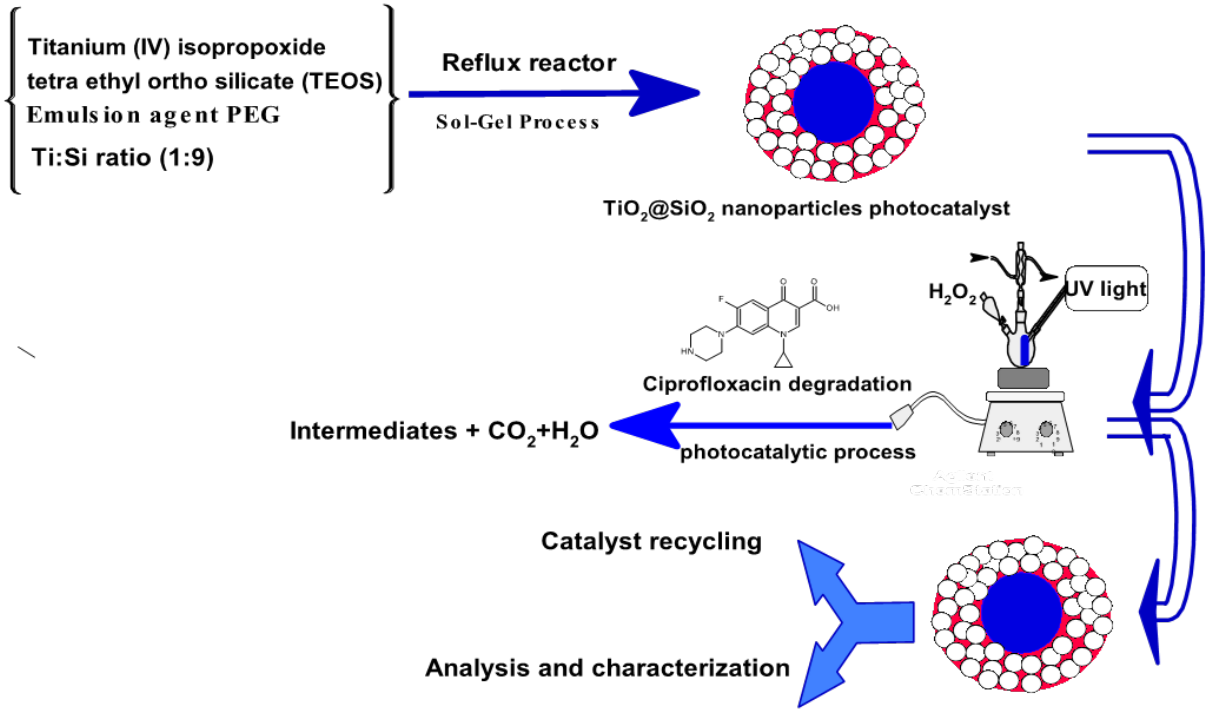

Figure 1. Illustration of photocatalytic oxidation of ciprofloxacin via TiO_2@SiO_2 nanocomposite.

solutions were prepared at 10 mg/L concentration by dissolving accurately weighed amounts of the antibiotic in ultrapure water (pH of 5.5-6.5) under constant stirring to ensure complete dissolution.

2.2 Analytical Instrumentation

Fourier-transform infrared (FTIR) spectra were recorded on a Perkin-Elmer Spectrum Two spectrometer to identify functional groups and confirm the chemical structure of the synthesized materials. UV-visible absorption spectra were obtained using a Perkin-Elmer Lambda 25 UV-Vis spectrophotometer to monitor ciprofloxacin concentration changes during photocatalytic experiments. Measurements of pH were conducted with an Adwa AD1030 pH meter calibrated daily with standard buffer solutions. The morphology, topology and elemental composition of the TiO_2@SiO_2 nanocomposite, both before and after photocatalytic treatment, were examined by scanning electron microscopy coupled with energy-dispersive X-ray spectroscopy (SEM-EDX) at magnifications up to 6000× using a Perkin-Elmer TM1000 system. Particle size measurements were performed using a Rigaku Miniflex 600 diffractometer. X-rays are produced from a Cu-Kα radiation source (copper anticathode) with a wavelength of 1.5418 Å and an accelerating voltage of 40 kV with a current of 15 mA. Data acquisition software is MiniFlex Guidance, while data processing software is PDXL2. The scan was performed within an analysis range of ($2° < 2\theta < 80°$) with a step size in degrees (°) and an acquisition time in seconds or a speed of 5.0000 deg/min. Particle size is then calculated using Scherrer's formula [34]:

$$D_{hkl} = \frac{K.\lambda}{B_{hkl}.\cos\theta} \quad (1)$$

where D_{hkl} is the average crystallite size (nm) in the direction perpendicular to the lattice planes, hkl are the Miller indices of the planes being analysed, K is the crystallite-shape factor (0.9 for spherical particles), λ is the X-ray wavelength (0.15418 nm), B is full-width at half-maximum (FWHM) of the diffraction peak (rad), and θ is the Bragg angle (rad). The Bragg angle, θ = peak position/2. Textural properties, including specific surface area, pore volume, and pore size distribution, were evaluated by nitrogen adsorption-desorption isotherms measured at 77 K using a Micromeritics ASAP 2020 instrument.

2.3 Synthesis of TiO_2@SiO_2 Nanocomposite Photocatalyst

The TiO_2@SiO_2 nanocomposite photocatalyst was synthesized via sol-gel method following molar ratios of TiO_2:SiO_2 = 1:9 [35-37]. In the first step, 0.10 moles of titanium (IV) isopropoxide were dissolved in 50 mL of 2-propanol and stirred under low temperature reflux at approximately 75 °C to promote hydrolysis and partial condensation at reduced energy consumption. Simultaneously, in a separate reactor, 0.90 moles of tetraethoxysilane (TEOS) were dissolved in 100 mL of benign solvent ethanol and subjected to ultrasonic agitation for 30 minutes to ensure homogenous hydrolysis. Subsequently, 20 mL of polyethylene glycol (PEG) was added to the TEOS solution to act as a templating and stabilizing agent, and the mixture was stirred continuously for another 30 minutes.

The titanium precursor solution was then added dropwise into the TEOS/PEG mixture under ultrasonic irradiation for 60 minutes to promote thorough mixing and co-condensation. The resulting sol was left to undergo gelation overnight at room temperature in a sealed quartz reactor. After gel formation, the wet gel was repeatedly washed with ultrapure water and ethanol to remove unreacted species and impurities. The cleaned gel was then dried under ambient conditions and calcined at 400 °C for 24 hours in air to achieve crystallization of the TiO_2 phase and removal of organic residues. The final TiO_2@SiO_2 nanocomposite powder was further washed with ultrapure water and ethanol prior to its application in ciprofloxacin photocatalytic degradation experiments.

2.4 Photocatalytic Oxidation of Ciprofloxacin on TiO_2@SiO_2 Nanocatalyst

Photocatalytic experiments were conducted in a 500 mL sealed, cylindrical, batch glass reactor (10 cm diameter, 15 cm height) equipped with magnetic stirring at 300 rpm. The reactor was irradiated using Pen-Ray UV lamps (Model 1115, 25 W, 18 mA) placed 5 ± 0.56 cm from the reactor wall, providing an intensity of 12.5 ± 2.5 mW cm^{-2} at the solution surface, as calculated using Inverse Square Law in Equation (2):

$$I_2 = I_1 \times \left(\frac{d_1}{d_2}\right)^2 \quad (2)$$

where I is the light intensity and d is the distance between the light source and the irradiated surface. The lamps emitted primary wavelengths at 365 nm (UVA) and 254 nm (UVC), which were used in separate experimental sets. For each run, 0.25 g of TiO_2@SiO_2 photocatalyst was dispersed in 500 mL of an aqueous ciprofloxacin solution with an initial concentration of 10 $mg.L^{-1}$ (pH ~5.6 unless otherwise adjusted for pH studies).

Aliquots were withdrawn at predetermined time intervals and immediately subjected to centrifugation, followed by filtration to separate the photocatalyst particles, ensuring accurate measurement of the residual ciprofloxacin concentration in the solution. The pH of the

reaction mixture was continuously monitored using an Adwa AD1030 pH meter to maintain optimal photocatalytic conditions. The concentration of ciprofloxacin was quantitatively analyzed by UV-visible spectrophotometry, measuring the absorbance at 277 nm. Each experiment was conducted in triplicate to ensure reproducibility and statistical reliability.

The degradation efficiency (%) of ciprofloxacin was calculated according to Equation (3):

$$Degradation\ Efficiency\ (\%) = \left(\frac{C_0 - C_t}{C_0}\right) \times 100\% \quad (3)$$

where C_0 and C_t are the initial and time-bound concentrations of ciprofloxacin in the aqueous phase (mg.L^{-1}). To elucidate the reaction kinetics, the photocatalytic degradation data were modeled using the Langmuir–Hinshelwood (L–H) kinetic framework, which describes surface-mediated reactions on heterogeneous catalysts. The reaction rate is expressed as in the Equation (4):

$$r_0 = -\frac{dC_{ciprofloxacin}}{dt} = \frac{k_r K C_{eq}}{1 + K C_{eq}} \quad (4)$$

where r_0 is the initial rate in mg.L^{-1}·min^{-1}, k_r is the rate constant, K is the adsorption constant, and C_{eq} is the equilibrium concentration of the ciprofloxacin.

3. Results and Discussion

3.1 Characterization and Analysis of TiO_2@SiO_2 Nanocomposites

The TiO_2@SiO_2 crystallite sizes were estimated from XRD analysis. Figure 2 shows overlapping peaks broadening at 2 θ_0 approximately 22° and 25°, correspond to amorphous SiO_2 matrix and TiO_2 small crystallites of anatase phase [101] respectively, with B around 2°. Employing Scherrer formula in Equation (1), the TiO_2 peak yielded an average crystallite size D_{101} = 3.97 nm.

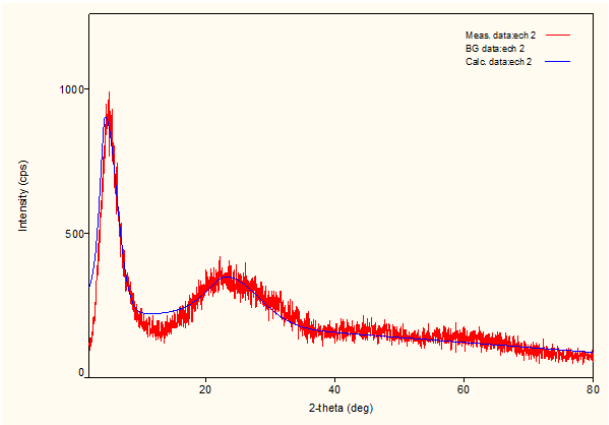

Figure 2. XRD analysis result of TiO_2@SiO_2 nanocatalyst.

The morphopological and topological characteristics of the TiO_2@SiO_2 nanocomposites were systematically investigated using SEM-EDX. This dual analytical technique enabled high-resolution imaging of the photocatalyst surface and concurrent elemental mapping to verify chemical composition. As shown in Figure 3a and 3b, the SEM micrographs reveal a heterogeneous and porous surface topology, featuring irregularly shaped crystalline aggregates and interconnected cavities of various sizes. The pores range from few tens to few hundred nanometers in diameter (Figure 4), forming a multi-scaled texture that favors enhanced mass transport and photon absorption for optimizing photocatalytic efficiency [38].

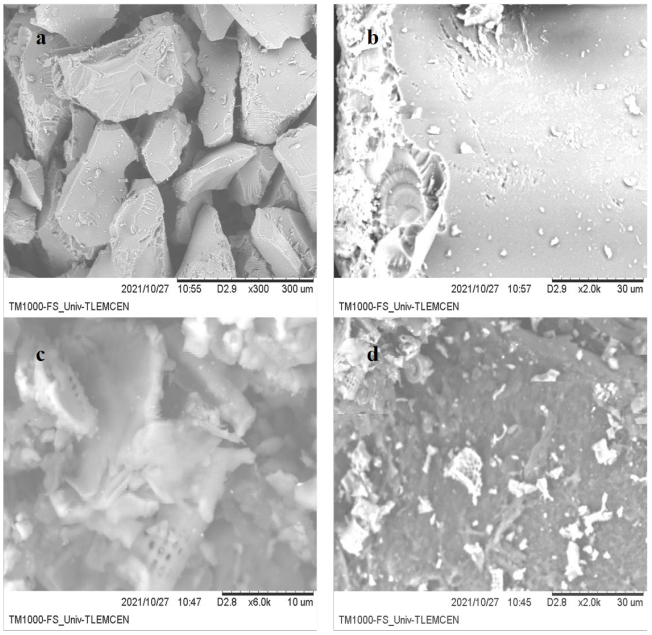

Figure 3. SEM micrographs of TiO_2@SiO_2 nanocomposites before (a and b) and after ciprofloxacin photodegradation (c and d).

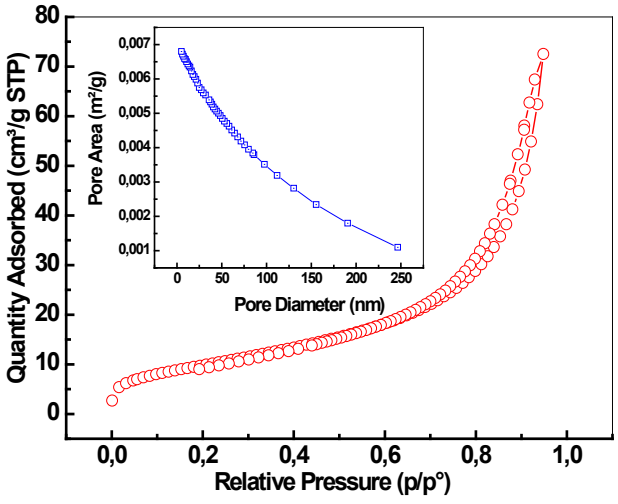

Figure 4. N_2 adsorption/desorption BET isotherms plot of TiO_2@SiO_2 nanocatalyst.

This macroporous structure, combined with a suitable pore dimension and robust topological stability, provides a favorable environment for photocatalytic reactions by increasing the density of active sites, facilitating reactant diffusion, and promoting light harvesting, rendering the TiO_2@SiO_2 nanocomposite a promising catalyst candidate for ciprofloxacin degradation under photocatalytic conditions.

Remarkably, post-degradation imaging of the catalyst following multiple photocatalytic cycles showed no discernible alteration in topology according to Figure 3c and 3d, indicating excellent structural integrity under operational stress [42]. This topological retention underscores the high mechanical and chemical stability of the TiO_2@SiO_2 system, aligning with the requirements for long-term use in water treatment applications [43].

Elemental analysis by EDX (Figure 5) confirmed the successful immobilization of TiO_2 nanoparticles onto the SiO_2 matrix. The Ti and Si peaks were prominently identified as a qualitative confirmation to the existence of Si-O-Ti bimetallic network after reaction. This compositional persistence of Si and Ti supports the recyclability and catalytic endurance of the composite material [44]. FTIR analysis (Figure 6) reveals surface interactions governing ciprofloxacin adsorption and degradation kinetics on TiO_2@SiO_2. The pristine catalyst shows characteristic Si–O–Si (1000–1200 cm^{-1}) and Ti–O/Ti–O–Si (400–800 cm^{-1}) bands [45]. After adsorption, changes indicate strong surface binding: broad O–H/N–H bands (3200–3600 cm^{-1}) shift and broaden due to hydrogen bonding, while the ciprofloxacin C=O stretch shifts from ~1700 cm^{-1} to 1680–1690 cm^{-1}, suggesting coordination to surface Ti^{4+}/Si^{4+} sites via Lewis acid–base interactions [46]. These adsorption mechanisms, hydrogen bonding, coordination, and electrostatic interactions, enhance surface coverage and favor the Langmuir–Hinshelwood kinetics observed, where initial degradation rates depend directly on adsorbed pollutant concentration.

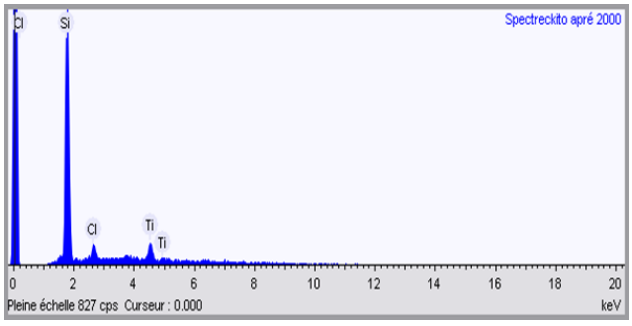

Figure 5. EDX elemental analysis results of TiO_2@SiO_2 nanocatalyst after reaction.

3.2. Kinetic Study on Ciprofloxacin Photodegradation

3.2.1 Effects of UV irradiation wavelength

Contact time is a pivotal parameter influencing both the efficiency and the underlying kinetics of ciprofloxacin photodegradation. The temporal evolution of ciprofloxacin degradation in the presence of TiO_2@SiO_2 nanocomposites under UV irradiation is illustrated in Figure 7a, 7b, and 7c, with the corresponding kinetic parameters summarized in Table 1. The kinetic parameters (r_0, k_r, K) and the linear correlation coefficient (R^2) calculated for both UVA and UVC light intensities (Table 1 and Figure 7b) were more adequate and suitable when following the pseudo-first-order

Table 1. Kinetic modelling parameters of ciprofloxacin photodegradation onto TiO_2@SiO_2 nanocomposite under various UV light wavelengths.

Kinetic Parameters	UV Wavelengths	
	254 nm	365 nm
r_0 (mg/L.min)	17.20	7.722
k_r	2.365	1.715
K	0.0050	0.0135
R^2	0.983	0.985

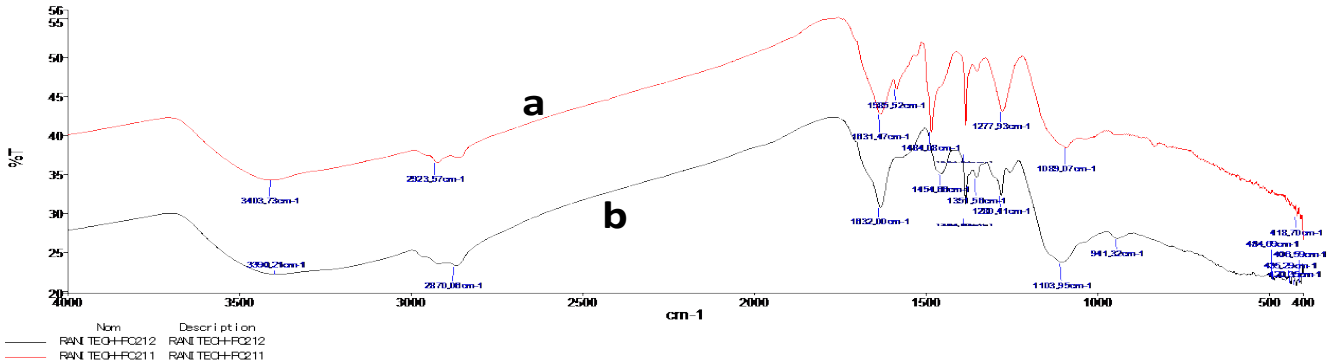

Figure 6. FTIR transmission spectra of TiO_2@SiO_2 photocatalyst before (a) and after (b) ciprofloxacin degradation.

model [47]. The calculated kinetic model data (mod) were very close to the experimental data (exp) as seen in Figure 7a.

The accuracy of this LH model fitting is also supported by R^2 values which are very close to unity. This observation suggests that the attenuation rate (represented by k_r) of ciprofloxacin depends on its concentration (r_0 = f(C_{eq})), with the adsorption process (represented by K) exhibiting wavelength-independent behavior, proving the effectiveness of the catalyst nanocomposite under various environmental conditions. TiO_2/SiO_2 nanocomposite shows considerable promise in ciprofloxacin photodegradation in aqueous medium.

The degradation efficiency, expressed as the concentration ratio (C_{eq}/C_0), decreased markedly from 0.9 to 0.1 over a period of 180 minutes, demonstrating the catalyst's robust photocatalytic performance in aqueous media (Figure 7c). During the initial phase (0–30 min), a rapid decline in

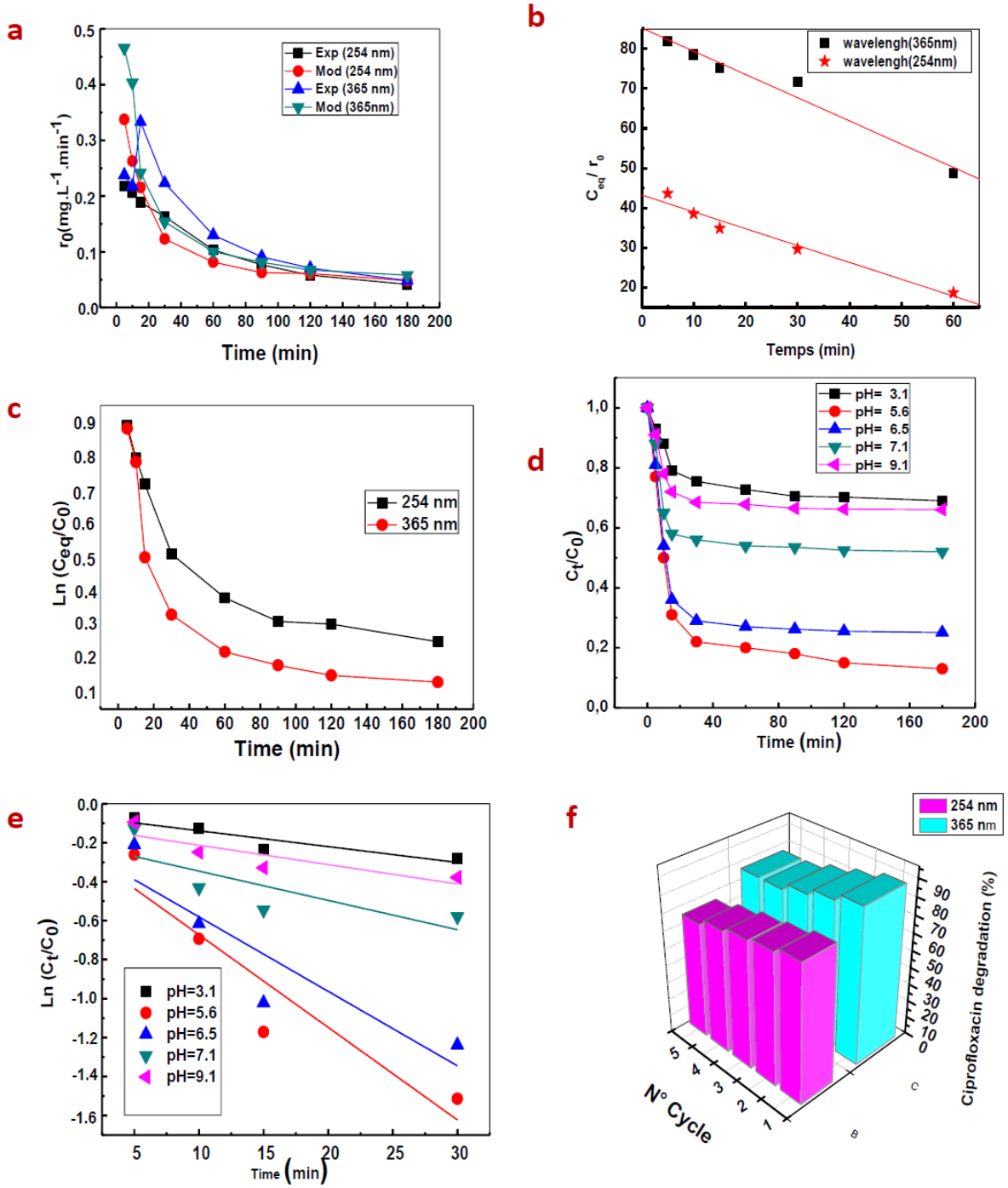

Figure 7. Kinetics analysis results: (i) Effects of UV irradiation wavelength and contact time on: (a) rate of reaction (exp: experimental; mod: model), (b) kinetic parameters and linear correlation, (c) degradation efficiency; (ii) Effects of pH and contact time on: (d) degradation efficiency, (e) kinetic parameters and linear correlation; (iii) Effects of UV irradiation wavelength and number of catalyst usage cycles on the rate of degradation.

ciprofloxacin concentration was observed. This accelerated degradation rate can be attributed to the abundance of accessible active sites on the TiO_2@SiO_2 surface, which promote effective adsorption of the pollutant and facilitate subsequent photogenerated charge transfer reactions [32,48]. Such behavior is consistent with Langmuir–Hinshelwood - based photocatalytic mechanisms, where surface saturation gradually occurs as active sites become occupied [30]. It appears that UVA irradiation leads to more complete mineralization with less hazardous intermediates. Moreover, UVA irradiation consumes lower energy than UVC, with higher potential of compatibility to solar-driven applications.

3.2.2 Effects of initial solution pH

The pH significantly influences ciprofloxacin degradation kinetics on TiO_2@SiO_2 (Figure 7d-e). Near-neutral conditions (pH of 5.6–6.5) maximize degradation, consistent with the pseudo-first-order kinetics observed in linearized plots (Figure 7e). At this pH, ciprofloxacin exists as a zwitterion ($pKa_1 \approx 6.1$, $pKa_2 \approx 8.7$), favouring electrostatic attraction to the partially deprotonated catalyst surface and enhancing adsorption, the rate-limiting step in Langmuir–Hinshelwood kinetics. Under strongly acidic (pH of 3.1) or alkaline (pH of 9.1) conditions, efficiency declines sharply due to electrostatic repulsion between the protonated (or deprotonated) catalyst and the antibiotic, and OH^- scavenging of hydroxyl radicals, respectively [29,31,49,50]. These results confirm that pH controls surface adsorption and radical availability, directly determining photocatalytic rate constants.

3.3. Catalyst Reusability and Photocatalytic Stability

Catalyst recyclability is a crucial criterion for assessing the efficiency and the practical performance of nanocomposite photocatalysts. After each photocatalytic cycle, the catalyst was recovered via centrifugation at 4000 rpm for 30 min, washed thoroughly with ultrapure water and ethanol, and dried at 80 °C for 2 h. To evaluate the long-term stability of TiO_2@SiO_2, the photocatalytic degradation of ciprofloxacin was conducted over five consecutive cycles under UV irradiations. As shown in Figure 7f, the degradation efficiency exhibited only a moderate decline from 89% to 77% under UVA irradiation (365 nm wavelength), and from 78% to 66% under UVC irradiation (254 nm wavelength). These results indicate that the photocatalyst retains a high level of activity over repeated uses, reflecting excellent mechanical stability, chemical resistance, and resistance to surface fouling.

The highest content of surface residue as observed after degradation belongs to Cl^- (Figure 5). Chloride anions are weakly bonded to the catalyst surface, and hence can be easily removed during catalyst recovery process. SEM micrographs in Figure 3c and 3d also show limited particle abrasion, inferring mechanical integrity of the nanocomposite structure. Such stability can be attributed to the structural integration of SiO_2, which enhances TiO_2 particle dispersion, inhibits agglomeration, and protects the photocatalytic sites against photo-corrosion and surface deactivation [51]. Therefore, TiO_2@SiO_2 emerges as a promising recyclable material for practical pharmaceutical wastewater treatment applications.

The observed deactivation can be attributed to progressive surface fouling by degradation intermediates [31,49,50] and weakly adsorbed Cl^- species (Figure 5), combined with potential photo-corrosion of TiO_2 sites under prolonged UV exposure, or Ti^{4+} leaching in acidic media [29]. The SiO_2 matrix effectively mitigates nanoparticle agglomeration and structural fatigue (Figure 3c-d), while also shielding TiO_2 from lattice oxidation and ion leaching. The greater relative loss under UVC compared to UVA suggests higher-energy photons may accelerate surface defect formation.

3.4 Optimization of Degradation Parameters Using Response Surface Methodology (RSM)

RSM is a powerful statistical method for designing practical researches and optimizing experimental parameters [52-53]. It helps in understanding the relationships between the response and the multiple independent parameters. In waste water treatment process, the design of experiments is indispensable for developing, improving, and controlling the process engineering. The photocatalytic oxidation yield of ciprofloxacin was investigated using a set of three different factors in a Box–Behnken design provided by RSM. RSM uses a statistical model [54] to describe the combination between the independent variables and the response (Figure 8). A second order polynomial equation is developed as in Equation (5):

$$Y = a_0 + \sum_{i=1}^{k} a_i X_i + \sum_{i=1}^{k} a_{ii} X_i^2 + \sum_{i=1}^{k} a_{ij} X_i X_j + \varepsilon \quad (5)$$

where Y (%) is the response (photodegradation efficiency), X_i, X_j are the independent variables, a_i, a_j, a_{ii}, a_{ij} represents the regression coefficients, and ε the error term.

Table 2 shows the photocatalytic degradation efficiency (%) of ciprofloxacin, respectively at 365 nm and 254 nm, knowing that the efficiency depends on three parameters: time (between 2

minutes and 180 minutes; pH between 3 and 9; temperature between 20 °C and 40 °C). From the variation of ciprofloxacin degradation parameters, it can be seen that time takes more effect compared to the other independent factors. The pH of medium takes effect more than temperature. It was noted in Table 2 that the neutral pH medium (6.0) has a higher degradation rate compared to the acidic (pH of 3.0) and basic (pH of 9.0) medium [55]. The degradation

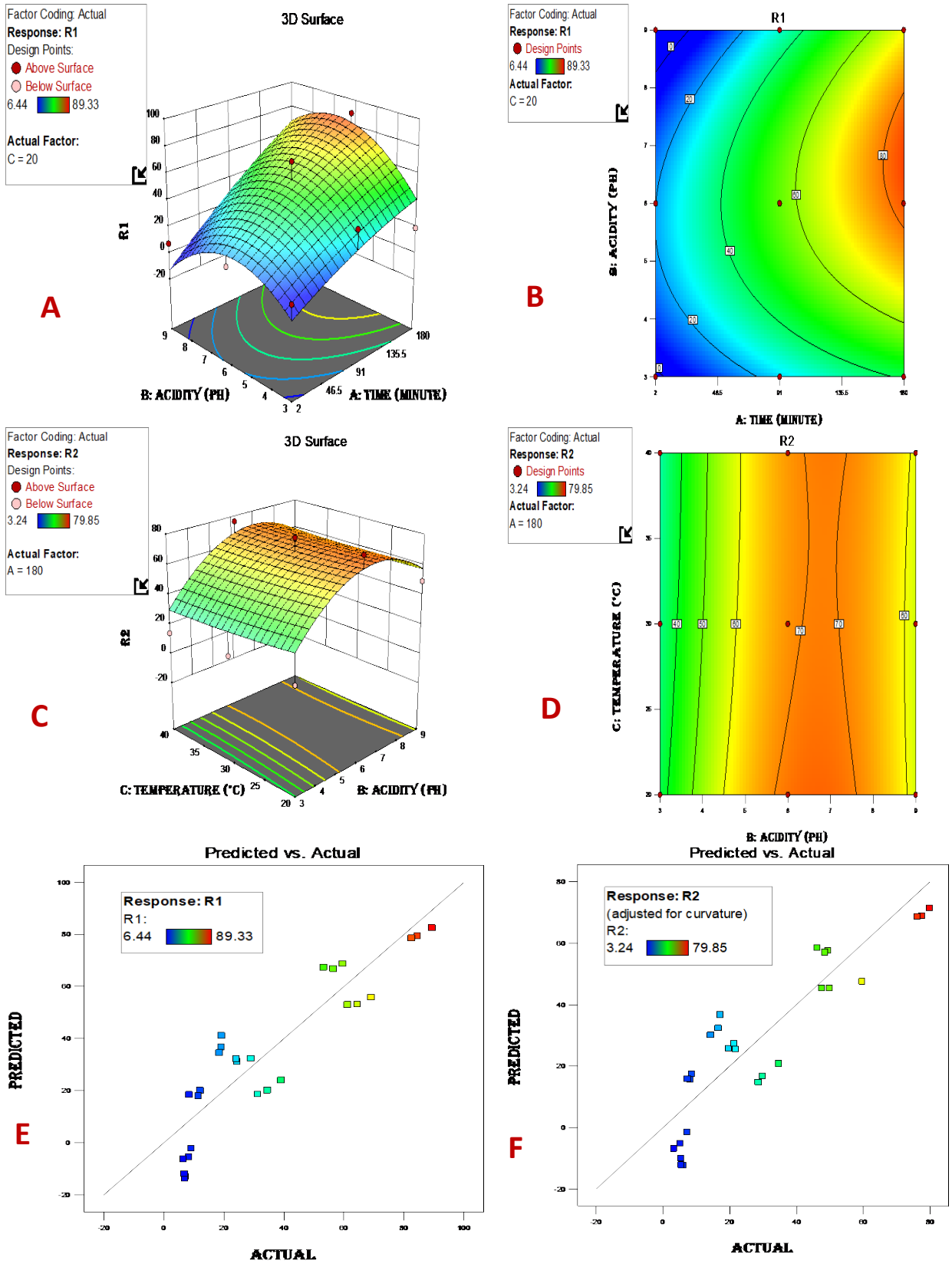

Figure 8. Response Surface Methodology (RSM) results for photocatalytic degradation efficiency (%) of ciprofloxacin: (i) response for UVA irradiation (R1) in: (a) 3D, (b) contour, and (e) comparison graphs; also (ii) response for UVC irradiation (R^2) in: (c) 3D, (d) contour, and (f) comparison graphs.

efficiency is optimal at 89.33% and 79.85% respectively for UVA and UVC irradiation, during 180 minutes degradation at 20 ºC and pH of 6.0. A decrease of the catalytic activity was verified in acidic and basic medium, as well as higher temperature up to 40 °C.

Based on the regression models provided in Table 2, the RSM results are presented in Figure 8 as three-dimensional (Figure 8a and 8c), contour (Figure 8b and 8d), and comparison (Figure 8e and 8f) graphs, contrasting the response of UVA (Figure 8a, 8b, 8e) and UVC (Figure 8b, 8d, 8f) irradiations. Figure 8a and 8b shows that irradiation time exerts more significant influence on the degradation efficiency compared to pH at a constant low temperature. Figure 8c and 8d shows that pH demonstrates more apparent effects on the degradation efficiency compared to temperature at a constant long irradiation time. The responses to the 2 irradiation wavelengths of UVA and UVS shows no significant contrast, as no apparent differences observed in Figure 8e and 8f, and no significant differences in F- and p-values obtained from Table 3. The analysis of the RSM

Table 2. RSM modelling of ciprofloxacin photodegradation onto TiO_2@SiO_2 nanocomposite under 2 UV light wavelengths using 3 input factors.

Run No.	Time (min)	pH	Temperature (°C)	Degradation efficiency (%)	
				UVA Irradiation (365 nm)	UVC Irradiation (254 nm)
1	2	3	20	9.1	7.2
2	2	3	30	8.3	5.14
3	2	3	40	6.44	3.24
4	2	6	20	12.10	8.55
5	2	6	30	11.45	8.11
6	2	6	40	8.44	7.33
7	2	9	20	7.22	6.11
8	2	9	30	6.98	5.44
9	2	9	40	6.88	5.33
10	91	3	20	39.05	34.6
11	91	3	30	34.53	29.8
12	91	3	40	31.22	28.55
13	91	6	20	69.05	59.6
14	91	6	30	64.53	49.8
15	91	6	40	61.22	47.52
16	91	9	20	29.05	19.6
17	91	9	30	24.43	21.8
18	91	9	40	24.11	21.22
19	180	3	20	19.2	17.1
20	180	3	30	19.11	16.52
21	180	3	40	18.55	14.25
22	180	6	20	89.33	79.85
23	180	6	30	84.5	77.5
24	180	6	40	82.54	76.15
25	180	9	20	59.66	49.33
26	180	9	30	56.5	48.5
27	180	9	40	53.23	46.22

$$R1\ (365\ nm) = -63.44251 + 0.252514*Time + 34.03103*pH - 1.06956*Temperature + 0.035983*Time*pH - 0.000675*Time*Temperature + 0.043479*pH*Temperature - 0.000570*Time^2 - 3.06505*pH^2 + 0.012196*Temperature^2$$

$$R2\ (254\ nm) = -51.57458 + 0.204648*Time + 29.19664*pH - 1.09129*Temperature + 0.029613*Time*pH - 0.000346*Time*Temperature + 0.063801*pH*Temperature - 0.000396*Time^2 - 2.69439*pH^2 + 0.010505*Temperature^2$$

results indicates that the optimization of some factors like pH and irradiation time resulted in fast and significant ciprofloxacin degradation. The ANOVA analysis test presented in Table 3 indicates that the response surface model is significant. The F-value of 8.16 implies the model is significant for the response R1 (365 nm) (the p-value = 0.0002 is < 0.0500). On the other hand, the response R2 (254 nm) indicates also a significant model according to the ANOVA analysis (the F-value = 6.42, and the p-value = 0.0007 is < 0.0500). This finding is also supported by the predictive power of the regression model (R1 and R2) as indicated in Figure 8e and 8f by the close proximity of all the predicted and actual response values to the diagonal line, which slope represents the correlation coefficient (R^2 and Adj-R^2) = 1.

4. Conclusions

This work introduces a green-synthesized TiO_2@SiO_2 hydrogel nanocomposite as a highly efficient, and stable photocatalyst for ciprofloxacin degradation. By systematically optimizing the process via RSM, we identified UVA (365 nm) irradiation and near neutral pH as key factors, achieving ~90% degradation, – surpassing conventional UVC -driven systems. The reaction adhered to pseudo-first-order Langmuir-Hinshelwood kinetics, with rapid initial degradation, confirming effective surface adsorption and radical-mediated oxidation. The catalyst retained >77% activity over five reuse cycles, attributable to the SiO_2 matrix, which prevents TiO_2 agglomeration, mitigates photo-corrosion, and enhances charge separation. This study advances photocatalytic material design by coupling green synthesis with UVA-focused, RSM-optimized operation, offering a scalable, energy-efficient alternative to traditional high-energy AOPs. Practically, this system demonstrates strong potential for solar-compatible, low-cost water treatment. Future effort should focus on solar- photoreactor integration, continuous-flow operation, and remediation of complex antibiotic-laden wastewaters to transition this technology toward real-world application.

Acknowledgment

This research was supported and funded by University Center Salhi Ahmed Naama (Algeria), Laboratory of Inorganic Chemistry and Environment, and Department of Chemistry (Tlemcen University). Generative AI is used in the writing process to improve the readability of the manuscript.

CRedit Author Statement

Author Contributions: R. Mansour: methodology, formal analysis, and data curation; N. Ferrah: conceptualization, project administration, and writing original draft; N.H. Fithriyah, I. Purnawan, M. Chabane: writing review and editing; F. Zahouane: experimentation, methodology, and software validation; C. Melkaoui: methodology and resources. All authors have read and agreed to the published version of the manuscript.

Table 3. ANOVA analysis and factors values for quadratic model of ciprofloxacin photodegradation onto TiO_2@SiO_2 nanocomposite under 2 UV light wavelengths.

Factor	Name	Medium Level	Low Level	High Level	Std. Dev.	Coding
A	Time	91.00	2.00	180.00	0.0000	Actual
B	pH	6.00	3.00	9.00	0.0000	Actual
C	Temperature	30.00	20.00	40.00	0.0000	Actual
Response 1: UVA Irradiation (365 nm)	Sum of Squares	df	Mean Square	F-value	p-value	Remarks
Blocks	4055.55	1	4055.55			
Model	12419.23	9	1379.91	8.16	0.0002	significant
Residual	2707.11	16	169.19			
Response 2: UVC Irradiation (254nm)	Sum of Squares	df	Mean Square	F-value	p-value	Remarks
Blocks	3690.38	1	3690.38			
Model	9153.40	9	1017.04	6.42	0.0007	significant
Residual	2534.06	16	158.38			

References

[1] Chen, P., Gou, Y., Ni, J., Liang, Y., Yang, B., Jia, F., Song, S. (2020). Efficient Ofloxacin degradation with Co (Ⅱ)-doped MoS_2 nano-flowers as PMS activator under visible-light irradiation. *Chemical Engineering Journal*, 401, 125978. DOI: 10.1016/j.cej.2020.125978

[2] Du, Z., Li, K., Zhou, S., Liu, X., Yu, Y., Zhang, Y., He, Y., Zhang, Y. (2020). Degradation of ofloxacin with heterogeneous photo-Fenton catalyzed by biogenic Fe-Mn oxides. *Chemical Engineering Journal*, 380, 122427. DOI: 10.1016/j.cej.2019.122427

[3] Gutiérrez-Sánchez, P., Álvarez-Torrellas, S., Larriba, M., Gil, M.V., Garrido-Zoido, J.M., García, J. (2023). Efficient removal of antibiotic ciprofloxacin by catalytic wet air oxidation using sewage sludge-based catalysts: Degradation mechanism by DFT studies. *Journal of Environmental Chemical Engineering*, 11(2), 109344. DOI: 10.1016/j.jece.2023.109344

[4] Pal, D., Pal, T., Pal, A. (2024). Efficient catalytic degradation of ciprofloxacin in synthetic and real wastewater under aerobic condition using microporous ammonium phosphomolybdate. *Journal of Water Process Engineering*, 63, 105382. DOI: 10.1016/j.jwpe.2024.105382

[5] Zhang, Y., Zhao, W., Zhang, X., Wang, S. (2024). Highly efficient targeted adsorption and catalytic degradation of ciprofloxacin by a novel molecularly imprinted bimetallic MOFs catalyst for persulfate activation. *Chemosphere*, 357, 141894. DOI: 10.1016/j.chemosphere.2024.141894

[6] Ferrah, N., Merghache, D., Lebar, G. (2022). Al_2O_3@ SiO_2-chitosan synthesis via sol–gel process and its application for ciprofloxacin adsorption. *Desalination and Water Treatment*, 255, 136-144. DOI: 10.5004/dwt.2022.28334

[7] Fick, J., Söderström, H., Lindberg, R.H., Phan, C., Tysklind, M., Larsson, D.J. (2009). Contamination of surface, ground, and drinking water from pharmaceutical production. *Environmental Toxicology and Chemistry*, 28(12), 2522-2527. DOI: 10.1897/09-073.1

[8] Hiller, C., Hübner, U., Fajnorova, S., Schwartz, T., Drewes, J. (2019). Antibiotic microbial resistance (AMR) removal efficiencies by conventional and advanced wastewater treatment processes: A review. *Science of the Total Environment*, 685, 596-608. DOI: 10.1016/j.scitotenv.2019.05.315

[9] López-Serna, R., Kasprzyk-Hordern, B., Petrović, M., Barceló, D. (2013). Multi-residue enantiomeric analysis of pharmaceuticals and their active metabolites in the Guadalquivir River basin (South Spain) by chiral liquid chromatography coupled with tandem mass spectrometry. *Analytical and Bioanalytical Chemistry*, 405(18), 5859-5873. DOI: 10.1016/j.apsusc.2019.06.123

[10] Petrie, B., Barden, R., Kasprzyk-Hordern, B. (2015). A review on emerging contaminants in wastewaters and the environment: current knowledge, understudied areas and recommendations for future monitoring. *Water Research*, 72, 3-27. DOI: 10.1016/j.watres.2014.08.053

[11] Vedenyapina, M., Kurmysheva, A.Y., Rakishev, A., Kryazhev, Y.G. (2019). Activated carbon as sorbents for treatment of pharmaceutical wastewater. *Solid Fuel Chemistry*, 53, 382-394. DOI: 10.3103/S0361521919070061

[12] Armaković, S.J., Armaković, S., Šibul, F., Četojević-Simin, D.D., Tubić, A., Abramović, B.F. (2020). Kinetics, mechanism and toxicity of intermediates of solar light induced photocatalytic degradation of pindolol: Experimental and computational modeling approach. *Journal of Hazardous Materials*, 393, 122490. DOI: 10.1016/j.jhazmat.2020.122490

[13] Song, J., Zhao, C., Cao, X.-q., Cheng, W. (2023). Enhanced catalytic degradation of antibiotics by peanut shell-derived biochar-Co_3O_4 activated peroxymonosulfate: An experimental and mechanistic study. *Process Safety and Environmental Protection*, 171, 423-436. DOI: 10.1016/j.psep.2023.01.036

[14] Yang, R., Wang, Z., Guo, J., Qi, J., Liu, S., Zhu, H., Li, B., Liu, Z. (2024). Catalytic degradation of antibiotic sludge to produce formic acid by acidified red mud. *Environmental Research*, 245, 117970. DOI: 10.1016/j.envres.2023.117970

[15] Sezer, S., Demircivi, P., Aydin, N.E., Saygili, G.N. (2024). Photocatalytic degradation of ciprofloxacin by using tannin-doped $BaTiO_3$ catalyst. *Journal of Photochemistry and Photobiology A: Chemistry*, 451, 115468. DOI: 10.1016/j.jphotochem.2024.115468

[16] Singh, P.P., Pandey, G., Murti, Y., Gairola, J., Mahajan, S., Kandhari, H., Tivari, S., Srivastava, V. (2024). Light-driven photocatalysis as an effective tool for degradation of antibiotics. *RSC Advances*, 14(29), 20492-20515. DOI: 10.1039/D4RA03431G

[17] Zha, Y., He, X., Wang, Y., Chen, W., Chen, L., Chen, L., Wang, S., Yan, B., Ma, B., Li, J. (2024). Visible-light-response Fe-doped BiOCl microspheres with efficient photocatalysis-Fenton degradation of antibiotics. *Journal of Water Process Engineering*, 67, 106225. DOI: 10.1016/j.jwpe.2024.106225

[18] Pham, T.-D., Hanh, N.T., Khoa, N.V., Van Noi, N., Cam, N.T.D., Ngoc, H.M., Thao, P., Trang, H.T., Huong, N.T. (2025). Optimization of photocatalysis using vanadium doped WO_3 under visible light to completely eliminate residual antibiotics in aqueous environment. *Journal of Photochemistry and Photobiology A: Chemistry*, 462, 116243. DOI: 10.1016/j.jphotochem.2024.116243

[19] Shi, Y., Hu, Y., Cheng, J., Zhu, X., Wang, G., Xie, J. (2024). Efficient degradation of ciprofloxacin by 3D oxygen-doped MoS_2/polyacrylamide/graphene oxide composite hydrogel co-catalytic Fenton reaction. *Journal of Environmental Chemical Engineering*, 12(1), 111759. DOI: 10.1016/j.jece.2023.111759

[20] Yang, J., Xu, M., Qin, M., Li, P., Liu, H. (2024). Co (CO_3) 0.5 (OH)• 0.11 H_2O as superior peroxymonosulfate activator for ciprofloxacin degradation via co-acting mechanism of low & high-valent cobalt and oxygen vacancy. *Journal of Environmental Chemical Engineering*, 12(1), 111872. DOI: 10.1016/j.jece.2024.111872

[21] Hu, Y., Jiang, L., Zhang, T., Jin, L., Han, Q., Zhang, D., Lin, K., Cui, C. (2018). Occurrence and removal of sulfonamide antibiotics and antibiotic resistance genes in conventional and advanced drinking water treatment processes. *Journal of Hazardous Materials*, 360, 364-372. DOI: 10.1016/j.jhazmat.2018.08.012

[22] Dai, P., Wu, M., Jiang, T., Hu, H., Yu, X., Bai, Z. (2018). Silver-loaded ZnO/$ZnFe_2O_4$ mesoporous hollow spheres with enhanced photocatalytic activity for 2, 4-dichlorophenol degradation under visible light irradiation. *Materials Research Bulletin*, 107, 339-346. DOI: 10.1016/j.materresbull.2018.07.014

[23] Di Mauro, A., Fragalà, M.E., Privitera, V., Impellizzeri, G. (2017). ZnO for application in photocatalysis: From thin films to nanostructures. *Materials Science in Semiconductor Processing*, 69, 44-51. DOI: 10.1016/j.mssp.2017.03.029

[24] Qi, K., Cheng, B., Yu, J., Ho, W. (2017). Review on the improvement of the photocatalytic and antibacterial activities of ZnO. *Journal of Alloys and Compounds*, 727, 792-820. DOI: 10.1016/j.jallcom.2017.08.142

[25] Salah, N.H., Bouhelassa, M., David, B. (2011). Photocatalytic decoloration of Cibacron Green RG12, on TiO_2 fixed on mineral supports by the PMTP method. *Physics Procedia*, 21, 115-121. DOI: 10.1016/j.phpro.2011.10.017

[26] Ould-Mame, S., Zahraa, O., Bouchy, M. (2000). Photocatalytic degradation of salicylic acid on fixed TiO_2-kinetic studies. International Journal of Photoenergy, 2(2), 59-66. DOI: 10.1155/S1110662X0000009X

[27] Brinker, C.J., Scherer, G.W. (1990). *Sol-Gel Science: The Physics and Chemistry of Sol-Gel Processing*. San Diego: Academic Press. ISBN 978-0-08-057103-4. DOI: 10.1016/C2009-0-22386-5

[28] Danks, A.E., Hall, S.R., Schnepp, Z. (2016). The evolution of 'sol–gel' chemistry as a technique for materials synthesis. *Materials Horizons*, 3, 91-112. DOI: 10.1039/C5MH00260E

[29] Hu, X., Hu, X., Peng, Q., Zhou, L., Tan, X., Jiang, L., Tang, C., Wang, H., Liu, S., Wang, Y., Ning, Z. (2020). Mechanisms underlying the photocatalytic degradation pathway of ciprofloxacin with heterogeneous TiO_2. *Chemical Engineering Journal*, 380, 122366. DOI: 10.1016/j.cej.2019.122366

[30] Akter, S., Islam, M. S., Kabir, M.H., Shaikh, M. A.A., Gafur, M.A. (2022). UV/TiO_2 photodegradation of metronidazole, ciprofloxacin and sulfamethoxazole in aqueous solution: An optimization and kinetic study. *Arabian Journal of Chemistry*, 15(7), 103900. DOI: 10.1016/j.arabjc.2022.103900

[31] Dhiman, P., Sharma, J., Hatshan, M.R., Ghfar, A.A., Kumar, A., Sharma, G. (2024). Rare earth ions doping enhanced photocatalytic activity of Bi_5O_7I for superior visible light driven degradation of ciprofloxacin. *Water, Air, & Soil Pollution*, 235(12), 776. DOI: 10.1007/s11270-024-07570-y

[32] Guo, W., Cai, J., Zheng, Y., Xiang, W., Xu, J., Zhang, Y. (2025). One-step grinding significantly enhances the visible-light photocatalytic degradation of antibiotics in water by TiO_2-BiOBr: A comparative study. *Journal of Alloys and Compounds*, 181882. DOI: 10.1016/j.jallcom.2025.181882

[33] Tasisa, Y.E., Sarma, T.K., Krishnaraj, R., Sarma, S. (2024). Band gap engineering of titanium dioxide (TiO_2) nanoparticles prepared via green route and its visible light driven for environmental remediation. *Results in Chemistry*, 101850. DOI: 10.1016/j.rechem.2024.101850

[34] Holzwarth, U. Gibson, N. (2011). The Scherrer equation versus the 'Debye-Scherrer equation'. *Nature Nanotechnology*, 6, 534. DOI: 10.1038/nnano.2011.145

[35] Muñoz-Aguado, M.J., Gregorkiewitz, M., Larbot, A. (1992). Sol-gel synthesis of the binary oxide (Zr, Ti) O_2 from the alkoxides and acetic acid in alcoholic medium. *Materials Research Bulletin*, 27(1), 87-97. DOI: 10.1016/0025-5408(92)90046-3

[36] Rehspringer, J., Poix, P., Bernier, J. (1986). Synthesis of glass "precursor" BaO, TiO_2, nH_2O by gel processing. *Journal of Non-Crystalline Solids*, 82(1-3), 286-292. DOI: 10.1016/0022-3093(86)90143-2

[37] Wang, Y., Liu, H., Cheng, H., Wang, J. (2015). Fabrication and properties of 3D oxide fiber-reinforced Al_2O_3–SiO_2–SiOC composites by a hybrid technique based on sol–gel and PIP process. *Ceramics International*, 41(1), 1065-1071. DOI: 10.1016/j.ceramint.2014.09.029

[38] Mulko, L., Soldera, M., Lasagni, A.F. (2022). Structuring and functionalization of non-metallic materials using direct laser interference patterning: a review. *Nanophotonics*, 11(2), 203-240. DOI: 10.1515/nanoph-2021-0591

[39] Jawad, A.H., Hameed, B., Abdulhameed, A.S. (2023). Synthesis of biohybrid magnetic chitosan-polyvinyl alcohol/MgO nanocomposite blend for remazol brilliant blue R dye adsorption: solo and collective parametric optimization. *Polymer Bulletin*, 80(5), 4927-4947. DOI: 10.1007/s00289-022-04294-z

[40] Koli, V.B., Mavengere, S., Kim, J.-S. (2019). An efficient one-pot N doped TiO_2-SiO_2 synthesis and its application for photocatalytic concrete. *Applied Surface Science*, 491, 60-66. DOI: 10.1016/j.apsusc.2019.06.123

[41] Thommes, M., Kaneko K., Neimark, A.V., Olivier, J.P., Rodriguez-Reinoso, F., Rouquerol, J., Sing, K.S.W. (2015). Physisorpion of gases, with special reference to the evaluation of surface area and pore size distribution (IUPAC Technical Report). *Pure and Applied Chemistry*, 87(9-10), 1051-1069. DOI: 10.1515/pac-2014-1117

[42] Soni, P., Pal, B., Das, R.K. (2024). Influence of ß-CD and Ag deposition over TiO_2 towards photocatalytic oxidation of urea under solar irradiation. *Journal of Environmental Chemical Engineering*, 12(2), 112150. DOI: 10.1016/j.jece.2024.112150

[43] Tian, W.-J., Chen, H.-J., Zhao, L., Zheng, L.-L., Hu, Z.-N., Yang, Y.-L. (2023). Preparation of adsorptive TiO_2/SiO_2 core-shell nanospheres by ultrasonic-coupled alkali leaching process: Synergy of adsorption and photocatalysis towards 2, 4-dinitrophenol removal. *Colloids and Surfaces A: Physicochemical and Engineering Aspects*, 679, 132530. DOI: 10.1016/j.colsurfa.2023.132530

[44] Sakti, L.K., Eddy, D.R., Permana, M.D., Firdaus, M. L., Deawati, Y., Rahayu, I. (2024). Utilizing TiO_2 photocatalysis and natural SiO_2 superhydrophilicity synergy to improve self-cleaning activity in cotton fabric. *Cellulose*, 31(9), 5885-5898. DOI: 10.1007/s10570-024-05938-1

[45] da Fonseca, B.T., D'Elia, E., Siqueira Júnior, J. M., de Oliveira, S.M., dos Santos Castro, K.L., Ribeiro, E.S. (2021). Study of the characteristics and properties of the SiO_2/TiO_2/Nb_2O_5 material obtained by the sol–gel process. *Scientific Reports*, 11(1), 1106. DOI: 10.1038/s41598-020-80310-4

[46] Massoudinejad, M., Sadani, M., Gholami, Z., Rahmati, Z., Javaheri, M., Keramati, H., Sarafraz, M., Avazpour, M., Shiri, S. (2019). Optimization and modeling of photocatalytic degradation of Direct Blue 71 from contaminated water by TiO_2 nanoparticles: Response surface methodology approach (RSM). *Iranian Journal of Catalysis*, 9(2). DOI: 10.57647/IJC. URL: https://oiccpress.com/ijc/article/view/4038

[47] Aggarwal, D., Kaur, M., Bansal, S., Singhal, S. (2025). Fabrication of eco-friendly $NiFe_2O_4$ nanocatalysts via plant extract-mediated synthesis: kinetic and mechanistic insights into photocatalytic degradation of an anthraquinone dye and tetracycline antibiotic. *Journal of Molecular Structure*, 1319, 139365. DOI: 10.1016/j.molstruc.2024.139365

[48] Gupta, A., Kumar, D., Shukla, S., Lee, Y., Lee, S., Sharma, S.K. (2025). Photocatalytic Degradation of Antibiotic Ciprofloxacin Using TiO_2: Ag Nanograins. *Ceramics International*. DOI: 10.1016/j.ceramint.2025.06.113

[49] Jyoti, Singh, K., Kumar, A., Kumar, D., Sawini, Singh, S., Kumar, A., Khan, A., Malik, A., Chauhan, A. (2025). NiO/Ag hybrid nanostructures synthesized using amine-functionalized NiO nanoparticles: structural, defect chemistry, morphological, optical properties and photocatalytic activity towards ciprofloxacin drug. Journal of Materials Science: *Materials in Electronics*, 36(1), 31. DOI: 10.1007/s10854-024-14044-8

[50] Pourshaban-Mazandarani, M., Nasiri, A. (2024). Photocatalytic degradation of tetracycline in wastewater with bio-based matrix magnetic heterogeneous nanocatalyst: performance and mechanism study. *Journal of Polymers and the Environment*, 32(11), 5713-5737. DOI: 10.1007/s10924-024-03340-3

[51] Roushree, R., Haimbodi, R. (2025). Recent Advances in ZnO-Based Nanocomposites for Amoxicillin Photocatalytic Degradation and Adsorption in Wastewater: A Review. *Journal of Inorganic and Organometallic Polymers and Materials*, 1-38. DOI: 10.1007/s10904-025-03943-w

[52] Chellapandi, T., Sudharsan, S., Elamathi, M. (2025). Optimization strategies for norfloxacin photocatalytic degradation using response surface methodology and artificial neural network: a review. *Chemical Papers*, 1-16. DOI: 10.1007/s11696-025-04187-1

[53] Sahragard, S., Naghizadeh, A., Mortazavi-Derazkola, S., Derakhshani, E. (2024). Detoxification of Trimethoprim Antibiotic Using $NiFe_2O_4$@ MoO_3 Magnetic Nanocomposites Phyto-synthesized with Green Route: Experimental and RSM Modeling. *Bio Nano Science*, 14(2), 1119-1131. DOI: 10.1007/s12668-024-01420-1

[54] Samuel, H.M., Mecha, C.A., M'Arimi, M.M. (2024). Response surface methodology optimization of trimethoprim degradation in wastewater using Eosin-Y sensitized 25% $ZnFe_2O_4$-g-C_3N_4 composite under natural sunlight. *Reaction Kinetics, Mechanisms and Catalysis*, 137(4), 2415-2430. DOI: 10.1007/s11144-024-02650-w

[55] Meky, A.I., Hassaan, M.A., Fetouh, H.A., Ismail, A.M., El Nemr, A. (2024). Hydrothermal fabrication, characterization and RSM optimization of cobalt-doped zinc oxide nanoparticles for antibiotic photodegradation under visible light. *Scientific Reports*, 14(1), 2016. DOI: 10.1038/s41598-024-52430-8.